



CO₂-EOR Pilot Study on Deep Buried Low Permeability Hill Fracture Reservoir in Liaohe Oilfield

Xiao-ming Wu^{1,2(✉)}, Rui-zhi Luan¹, Ai-wu Yuan¹, Yu-ting Dai³, Fu-xing Zhang¹, Guo-bin Jiang⁴, and Zhen-yu Sun¹

¹ Liaohe Oilfield of CNPC, Panjin, China
wuming_fly@163.com

² College of Petroleum Engineering, China University of Petroleum, Panjin, China

³ College of Petroleum Engineering, Northeast Petroleum University, Daqing, China

⁴ Daqing Oilfield of CNPC, Daqing, China

Abstract. This is the first paper tells you how to design the well pattern and well spacing, how to optimize the injection and production parameters in buried hill fracture reservoir with great depth and low permeability. In addition, we also present the matched injection and production instruments developed for carbon dioxide flooding. All of these can provide reference and experience for this kind of reservoir.

We get exact parameters for simulation through different tests such as PVT tests, miscible experiments and displacement experiments. Then critical parameters such as well pattern, well spacing as also as injection-production rate are determined after analysis of field injection pilot date and numerical simulation with the test results. At the same time, wellhead injection pressure, injection tube diameter are got through calculation with software and dynamic corrosion tests in lab. Anti-gas lift technology through combination of gas anchor and unusual pump and corrosion protection facility by chemical agent are also developed to ensure success of pilot.

Laboratory experiment results show that oil volume expansion can reach 53.3% while viscosity reduces from 0.423 mPa·s to 0.221 mPa·s. Preliminary

Supported by CNPC CCUS Project, project number 2022ZS0805.

Copyright 2023, IFEDC Organizing Committee.

This paper was prepared for presentation at the 2023 International Field Exploration and Development Conference in Wuhan, China, 20–22 September 2023.

This paper was selected for presentation by the IFEDC Committee following review of information contained in an abstract submitted by the author(s). Contents of the paper, as presented, have not been reviewed by the IFEDC Technical Team and are subject to correction by the author(s). The material does not necessarily reflect any position of the IFEDC Technical Committee its members. Papers presented at the Conference are subject to publication review by Professional Team of IFEDC Technical Committee. Electronic reproduction, distribution, or storage of any part of this paper for commercial purposes without the written consent of IFEDC Organizing Committee is prohibited. Permission to reproduce in print is restricted to an abstract of not more than 300 words; illustrations may not be copied. The abstract must contain conspicuous acknowledgment of IFEDC. Contact email: paper@ifedc.org.

© The Author(s), under exclusive license to Springer Nature Singapore Pte Ltd. 2024

J. Lin (Ed.): IFEDC 2023, SSGG, pp. 418–433, 2024.

https://doi.org/10.1007/978-981-97-0268-8_33

injection tests show that the maximum daily injection rate is 60 t/d and absorption strength is 5.14 m³/(d.m) which is 6 times of water absorption strength. So we get the conclusion that effective displacement can be achieved and CO₂-EOR is feasible. Reversed nine-spot well pattern is adopted and the distance between injector and producer is 210 to 235 m which is reasonable for this kind of buried hill fracture reservoir and the predicted ultimate recovery is 40.05%. In the pilot, tube with Φ 73 mm diameter is used and designed injection rate is 30 t/d while wellhead pressure is 46.6 MPa which is basically the same to the calculation value. The pump setting depth is 2250 to 2440 m and combination anti-gas facility is adopted to meet the gas-oil ratio smaller up to 800, a critical factor to be considered. In the past one year, the number of effective wells accounts to 48% with daily production increased from 2 t/d to 8 t/d and the natural decline rate decreased from 26.1% to 6.9%. A satisfied pilot result has been got.

The paper introduces the parameters optimization, matched technology of field pilot and the pilot result that can provide a reference. CO₂-EOR way is an effective way for this kind of reservoir and can benefit to reduce carbon dioxide discharge.

Keywords: CCUS · deep buried low permeability hill fracture reservoir · Liaohe Oilfield

1 Introduction

As an effective measure to enhance oil recovery, CO₂ injection in heavy oil and thin oil can increase energy, reduce viscosity, expand sweep volume and improve oil displacement efficiency. These principles improve reservoir development effect. Especially for the bottom layer with high pressure, such as water injection and steam injection, it is difficult to replenish energy, so CO₂ injection is an effective way to improve oil recovery. Shuang 229 block of Liaohe Oilfield is a typical low permeability deep buried hill reservoir. High water injection pressure made the bottom energy unable to replenish, resulting in low oil recovery rate of 0.4% and recovery degree of 1.4%. This development block has great development potential, so we conducted a pilot test of CO₂ flooding. Meanwhile, we optimized development parameters and supporting injection-production process. The pilot test well group can bury 257,000 tons of CO annually and increase oil by more than 10,000 tons.

2 Overview of Block-229

Dawa Oilfield, Block 229 is located in Dawa District, Panjin City, Liaoning Province. On the plane of Block 229, there are four well areas: Shuang-229, Shuang-246, WA-128 and WA-111. The depth of the reservoir is 2900–3950 m. Accumulative reported proven petroleum geological reserves in the main strata is 2799.58×10^4 t. The reservoir space of oil reservoir is mainly composed of intergranular pores, intra-granular pores and granular dissolved pores. There are a small number of mold holes, microholes, and a small number of granular cracks, diagenetic microfractures. The effective porosity

was 12.7% and the permeability was 1.62 mD, the formation temperature is 99.33–129.88 °C, the temperature in the middle of the reservoir is 114 °C, the geothermal gradient is 3.03 °C/100 m, the formation pressure is 33.06–45.03 MPa, the formation pressure in the middle of the reservoir is 38.82 MPa, the pressure coefficient is 1.14, this is a normal temperature and pressure system.

Starting in 2016, a series of vertical well development systems have been developed in this area through pilot deployment, scale-up deployment, and overall deployment. Due to poor porosity and permeability characteristics, the well had a low production rate of 3.1 m³/d. Because energy is not replenished, production declines quickly after fracturing. With an annual decline rate of 40–55% and a predicted depletion recovery rate of only 7.5%, We need to find a way to replenish energy in order to enhance oil recovery. In 2023, we selected 6 well groups to conduct pilot tests of CO₂ flooding and achieved good results.

3 Injection Test and Analysis in Block-229

3.1 Water Injection Test

3.1.1 Formation Sensitivity Analysis

The sensitivity evaluation experiment of Wa-128 shows that: The rock samples have moderately strong water sensitivity, The salinity sensitive critical salinity is 7000 mg/l. The experimental results suggest that water quality should be controlled strictly and anti-swelling should be paid attention to in the process of waterflood development (Table 1).

Table 1. Statistical table of water sensitivity and salt sensitivity evaluation experiment of Shuang-229 Block Wa-128 well

sensitivity	Core signal	Well depth (m)	Gas permeability measurement (mD)	Permeability damage rate (%)	Degree of sensitivity
Water sensitivity	9	3736.79	2.42	67.8	Moderately
	15	3738.04	13.8	62.3	Moderately
Water sensitivity	9	3736.79	2.42	67.8	Critical salinity 7000 mg/l
	15	3738.04	13.8	62.3	Critical salinity 7000 mg/l

3.1.2 Starting Pressure Gradient Test

The initial water injection pressure of low permeability reservoir increases with the decrease of permeability. Test results of each block in Liaohe Oilfield show that the

average starting pressure gradient of water injection for permeable oil reservoir is less than 1.0 MPa/m. When permeability is less than 2.5 md, The starting pressure gradient increased greatly. The starting water injection pressure gradient measured in the laboratory experiment of Shuang229 well is as high as 1.49 MPa/m, and it is difficult to develop water injection system and establish displacement system.

Core displacement experiments show that Under the displacement pressure difference of 6–8 MPa and the injection multiple of more than 5 times, the displacement efficiency can reach 47%.

However, the actual injection volume in the field is between 0.5 and 1 PV, so the displacement efficiency is about 35%, and the reservoir displacement efficiency is relatively low (Figs. 1 and 2).

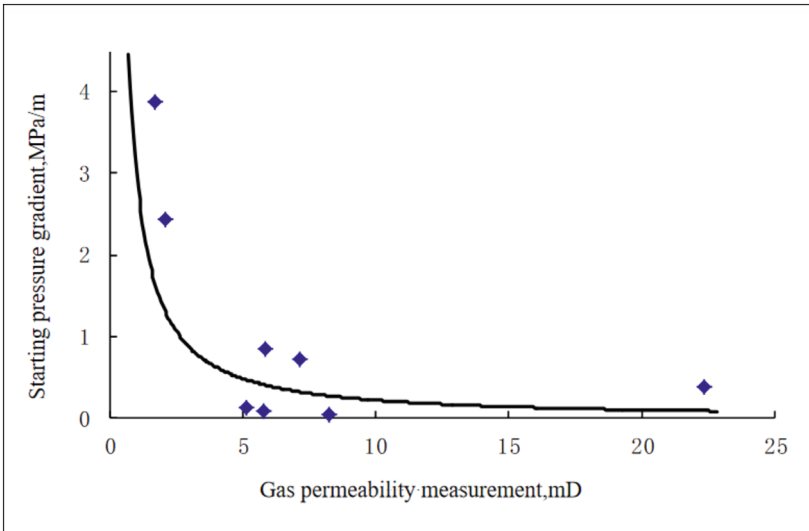


Fig. 1. Relationship between starting pressure gradient and permeability in Liaohe oilfield

3.2 Field Injection Test

3.2.1 Field Water Injection Test

Well Shuang-246 was put into trial injection on June 7, 2018. The water injection was 30 m³/d and the injection pressure was 17 MPa in the first days. Continuous injection was not possible after 6 days, and the average daily water injection after interinjection was 12.4 m³/d. The injection pressure was 25 MPa on July 31, and the injection water volume increased somewhat, but the injection pressure rose quickly. In the later period of injection, the daily injection was 14.1 m³/d. The injection stopped on September 11, and the cumulative injection was 1459 m³. The results of the injection test and the laboratory study are basically the same. Due to poor reservoir physical property, large seepage resistance, high water injection pressure, low water injection, it is difficult to reach the injection distribution (Fig. 3).

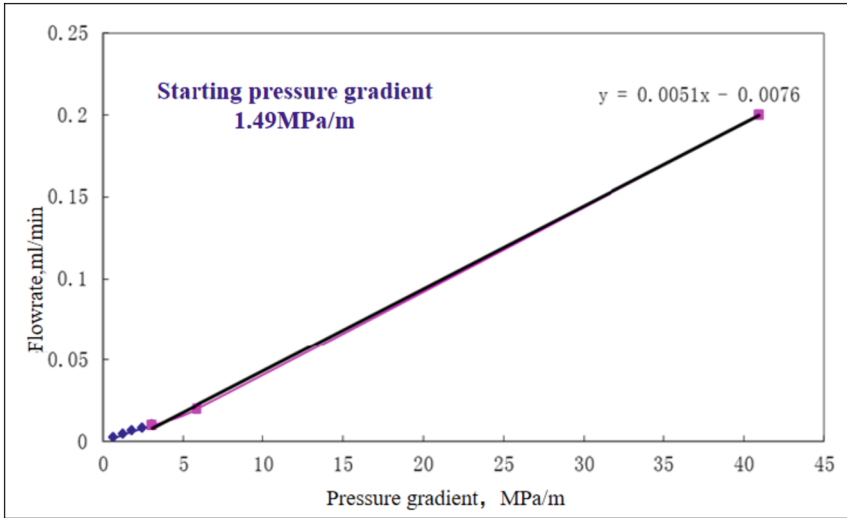


Fig. 2. Water injection seepage curve of rock sample of Shuang229 well (starting pressure gradient 1.49 MPa/m)

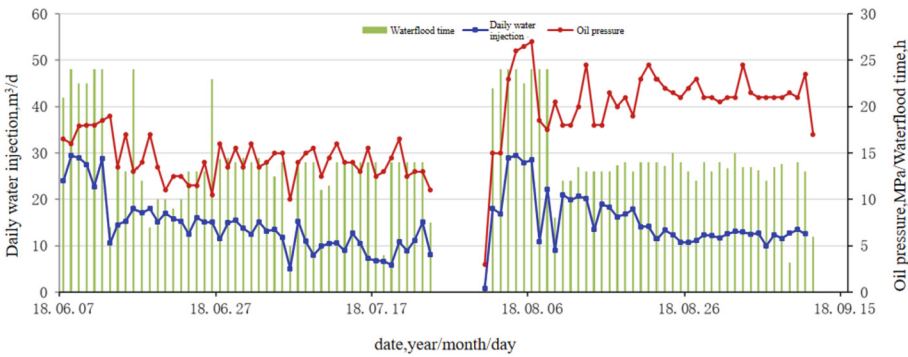


Fig. 3. Water injection test curve of Shuang246 well group

3.2.2 Field Nitrogen Injection Test

Since water injection is difficult and formation energy needs to be replenished, field tests of nitrogen injection are carried out. There were three test Wells on site, and their converted inspiratory strength was significantly better than that of water injection, and the formation energy was effectively supplemented, as shown in the Table 2.

Table 2. Statistical table of Shuang-229 gas injection well groups

Injection medium	Injection well	Horizon perforation	Thickness (m)	Maximum daily injection		Injection pressure (MPa)	water strength (Underground) (m ³ /(d.m))	Cumulative injection (10 ⁴ m ³)
				Ground (Nm ³)	Underground (m ³)			
water	Shuang-246	III group	20.7	28	28	27	1.35	0.1459
Nitrogen	Shuang-229-38-38	III group	17.4	40504	165	28.1	9.48	195.7
	Shuang-229-38-34	III IV group	36.9	59000	241	26.3	6.53	251.1
	Shuang-229-20-30	III IV group	11.7	28900	118	27	10.09	273.7

4 Carbon Dioxide Flooding

4.1 Feasibility Analysis of Carbon Dioxide Flooding

We screened nitrogen, air, carbon dioxide, and natural gas as alternatives, we test miscible pressure and displacement efficiency to determine suitable injection medium. The experimental results show that the minimum miscible pressures of carbon dioxide, natural gas, nitrogen and air are 31.8 MPa, 46.2 MPa, 62.1 MPa and 60.8 MPa, respectively. The core displacement experiments show that the displacement efficiencies of carbon oxide, natural gas, nitrogen and air are 81.3%, 70.1%, 54.9% and 60.4%. The formation pressure of Shuang229 reservoirs is 35.36–44.67 MPa, and the injection of natural gas and carbon dioxide can achieve mixed flooding. At the same time, considering the safety of development and the demand of carbon storage, carbon dioxide is selected as the displacement medium (Figs. 4, 5, 6, 7 and 8).

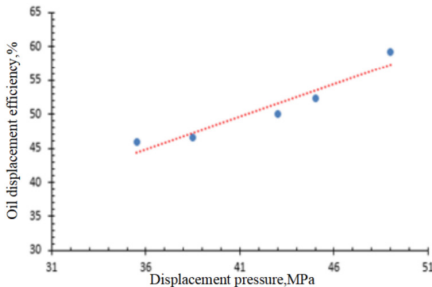


Fig. 4. Oil displacement efficiency of nitrogen injection under different displacement pressures

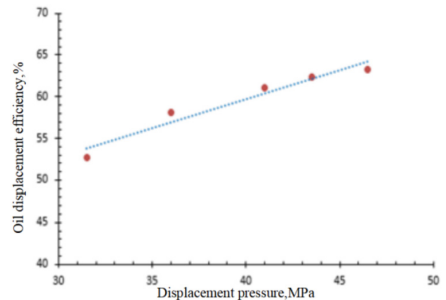


Fig. 5. Oil displacement efficiency of air injection under different displacement pressures

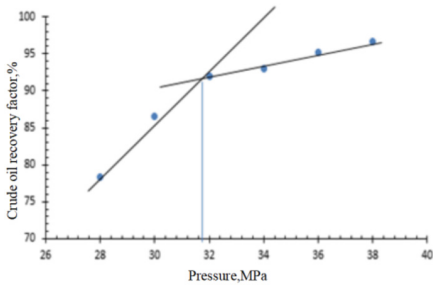


Fig. 6. Oil displacement efficiency of carbon dioxide injection under different displacement pressures

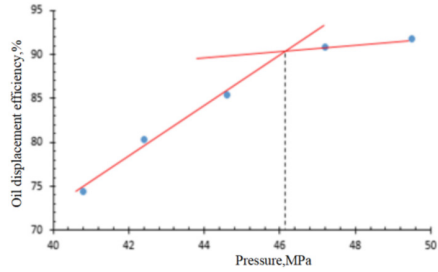


Fig. 7. Oil displacement efficiency of natural gas injection under different displacement pressures

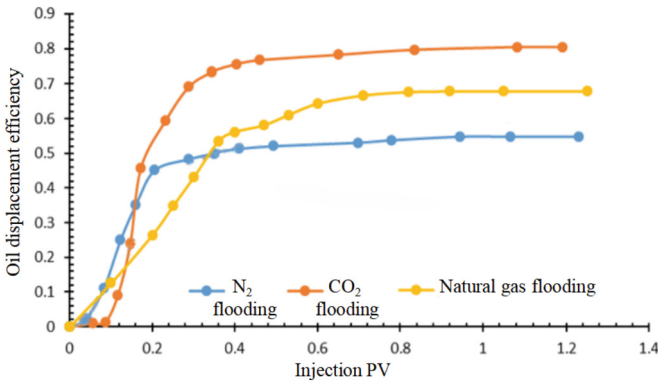


Fig. 8. Contrast curve of displacement efficiency of different media

4.2 Carbon Dioxide Flooding Mechanism

4.2.1 Viscosity Reduction

The oil swelling and viscosity reduction tests were carried out using 229 pairs of oil. The results showed that the oil swelling capacity of dissolved air, nitrogen, natural gas and CO₂ was 2.66%, 2.35%, 10.7% and 25.24%, respectively, at 41 MPa. The crude oil viscosity decreased from 0.423 mPa·s to 0.348 mPa·s, 0.354 mPa·s, 0.296 mPa·s and 0.221 mPa·s, respectively. Therefore, compared with other gases, CO₂ injection has the best swelling and viscosity reduction effect (Fig. 9).

4.2.2 Improved Oil Displacement Efficiency

The experimental results show that the miscible displacement efficiency of carbon dioxide can reach 81.3% through extraction, it greatly improves oil displacement efficiency. It has good applicability to the low permeability and deep buried hill reservoir in Shuang229 block (Fig. 10).

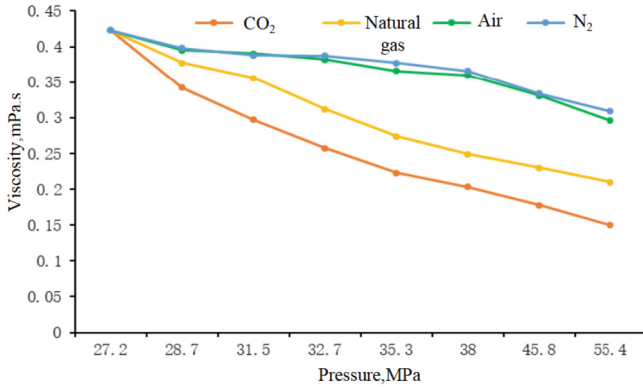


Fig. 9. The relationship between oil viscosity and pressure after injection of different gases

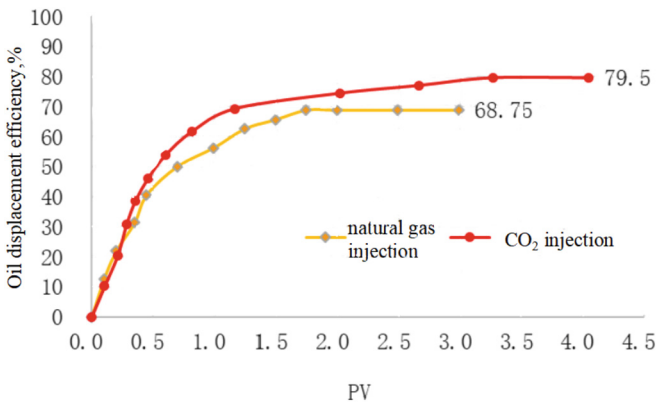


Fig. 10. Oil displacement efficiency curve of core displacement experiment with different injection media

4.3 Carbon Dioxide Flooding Parameters Design

The injection and production well pattern is diamond-shaped reversed nine-spot pattern. The spacing between injection and production Wells is 210–235 m. The formation pressure coefficient is maintained above 0.95, and the predicted recovery rate is 40.05% during the development cycle of 30 years (Table 3).

4.3.1 Injected PV Number

Experimental results show that the oil displacement efficiency increases by 16%, 6.5% and 2.5% when 0.5, 1.1, 1.5 and 2.0 HCPV are injected, respectively. It can be seen that after 1.5 HCPV, the gas-oil ratio doubled and the increase of oil displacement efficiency decreased (Fig. 11). Numerical simulation also shows that the recovery rate increases with the increase of injected PV number, and the recovery rate increases slowly after 1.5 HCPV injection. Therefore, 1.5 HCPV is determined as the injection PV number,

Table 3. Different injection-production well patterns and their advantages and disadvantages

Pattern type	Plan 1: rectangle at nine point	Plan 2: The diamond is reverse nine points
Injection-production well distance	210~420m	210~235m
Sample well pattern		
Number of injection-production Wells(Wa District 128)	5injectio24production	11injectio39production
Connectivity coefficient	51%~68%	60%~78%
Injection capacity	8.58×10^4 t/year	20.82×10^4 t/year
Recovery factor	cumulative injection1.0PV, recovery efficiency27%	cumulative injection1.5PV, recovery efficiency40%

which is the best development effect. In practice, circulation injection is adopted in the reservoir.

4.3.2 Injection Rate Optimization

Using the annual injection rate of 0.04, 0.06, 0.08, 0.1, 0.12 HCPV/a for simulation calculation, The comparative analysis shows that gas channeling will occur between oil Wells when the injection rate is higher than 0.08 HCPV/a. Oil production and stage recovery rate decreased significantly. Therefore, the reasonable gas injection rate is

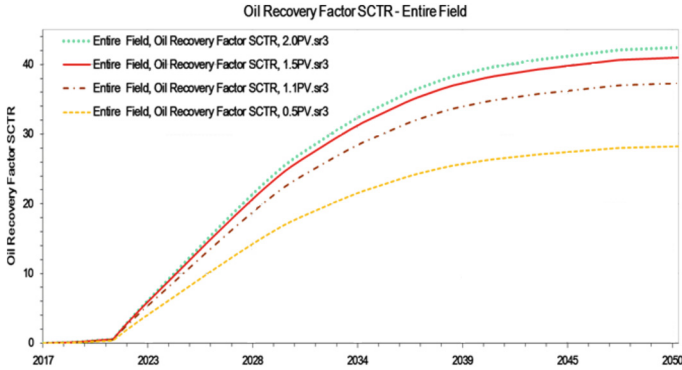


Fig. 11. Numerical model predicted recovery curve under different injected PV numbers

0.08 HCPV/a. The maximum daily injection gas of a single well is converted to 50 t/d, and the predicted wellhead injection pressure is 25 MPa and bottomhole flow pressure is 58 MPa, which is less than the reservoir fracture pressure (68 MPa) (Figs. 12 and 13).

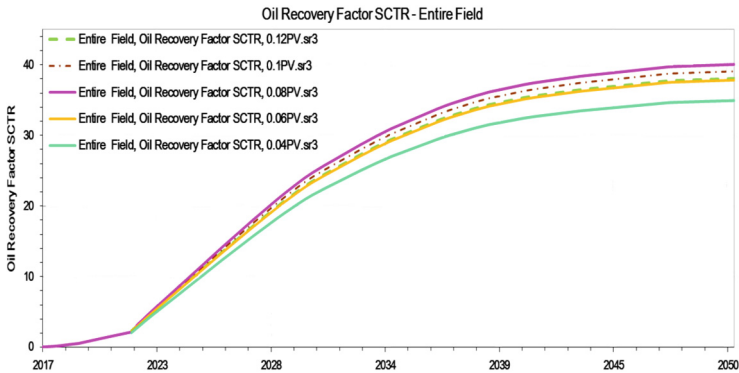


Fig. 12. Numerical model prediction of different gas injection velocity and recovery degree relationship curves

4.3.3 Influence of Injection Parameters on Bottom Hole Temperature and Pressure

Due to the great difference between liquid CO₂ and supercritical CO₂ flow in rock pores, it is very important to predict the phase state of CO₂ in the wellbore. The state relation of CO₂ phase is that its supercritical temperature is 31.26 °C and its supercritical pressure is 7.4 MPa. Phase state prediction can be converted into prediction of CO₂ temperature and pressure in the wellbore. Analysis of influence of injection pipe diameter on bottom hole temperature and pressure.

Analysis of Influence of Injection Pipe Diameter on Bottom Hole Temperature and Pressure. The wellbore flow prediction model is used to predict the wellbore pressure and

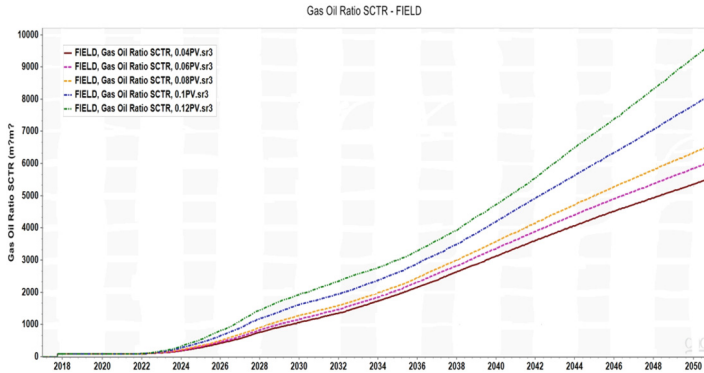


Fig. 13. Numerical model prediction of different gas injection velocity and gas - oil ratio curves

temperature of the commonly used $\Phi 50.8$ mm tubing, $\Phi 73$ mm tubing and $\Phi 88.9$ mm tubing under the conditions that the injection temperature is -18 °C, the injection pressure is 24 MPa and the injection volume is 50 m³/d. It can be seen from the predicted results that the change of pipe diameter has little influence on the pressure and temperature. Through analysis, CO₂ changes from liquid state to supercritical state at 1000 m inside the wellbore, and supercritical CO₂ has the fluidity similar to gaseous fluid and low friction along the pipe string, different pipe diameters have little influence on the final bottom hole pressure and temperature. Therefore, for the selection of CO₂ injection development pipe string, the testing and operation requirements of block development can be comprehensively considered first, and select the most economical applicable pipe diameter (Figs. 14 and 15).

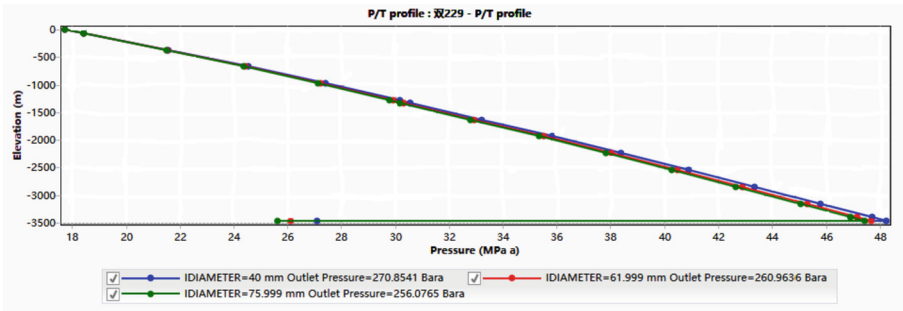


Fig. 14. Wellbore pressure prediction chart

Analysis of influence of injection rate on bottom hole temperature and pressure. Combined with the wellbore flow prediction model, under the conditions of injection speed of 20 t/d, 40 t/d, 60 t/d, 80 t/d and 100 t/d, injection temperature of -18 °C and injection pressure of 24 MPa, the tubing size of $\Phi 73$ mm was selected for wellbore pressure and temperature prediction. It can be seen from the predicted results that the

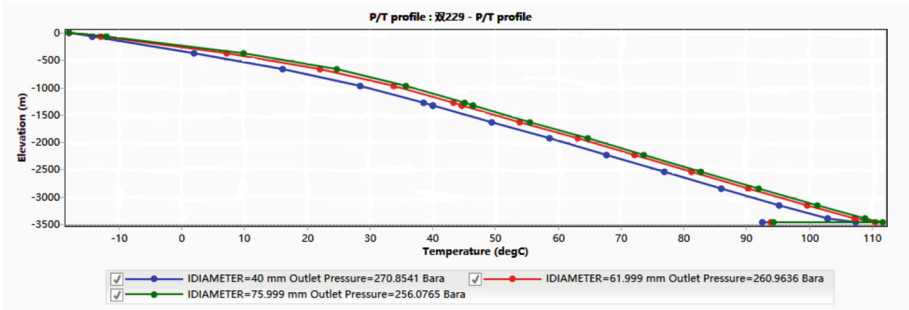


Fig. 15. Wellbore temperature prediction chart

injection rate has a great effect on the final bottomhole temperature and a small effect on the final bottomhole pressure (Figs. 16 and 17).

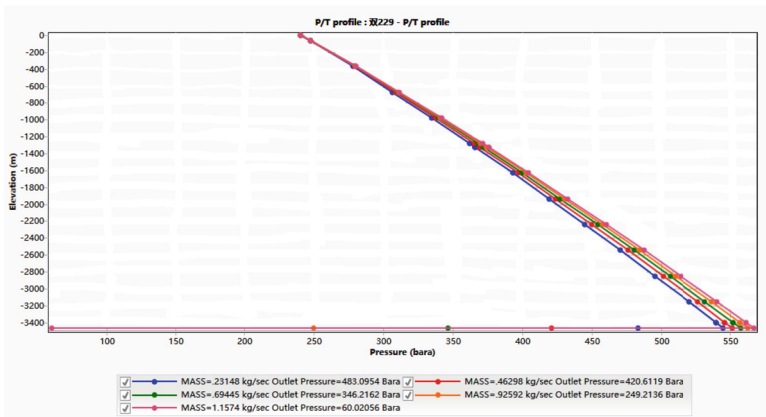


Fig. 16. Wellbore pressure prediction chart

Analysis of effect of injection phase on bottom hole phase. In order to study the influence of different injection methods on the final phase state of the bottom hole, combined with the wellbore flow prediction model, the wellbore pressure and temperature were predicted under the conditions of injection temperature of -18°C and 40°C and injection pressure of 24 MPa for the corresponding tubing when the injection speed was 20 t/d, 40 t/d, 60 t/d, 80 t/d and 100 t/d respectively. Compared with the liquid injection method, it can be seen that the final outlet pressure and temperature are basically the same, and the supercritical inflow can be realized, while the liquid injection has the advantages of strong technological applicability and low cost. Therefore, the liquid injection method has a lower cost for low permeability reservoirs above 2000 m (Figs. 18 and 19).

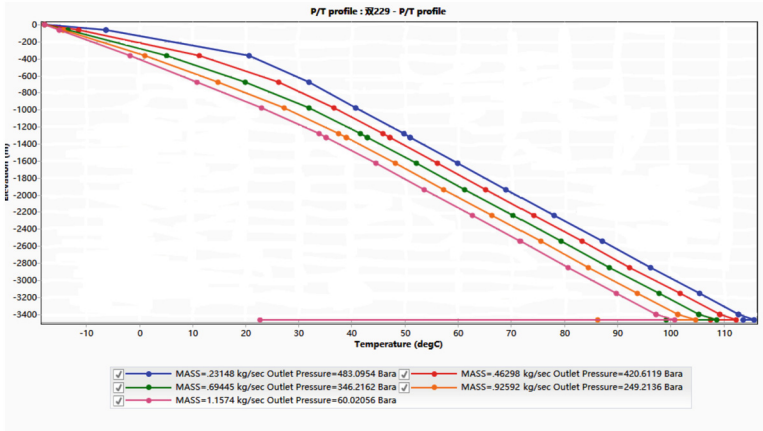


Fig. 17. Wellbore temperature prediction chart

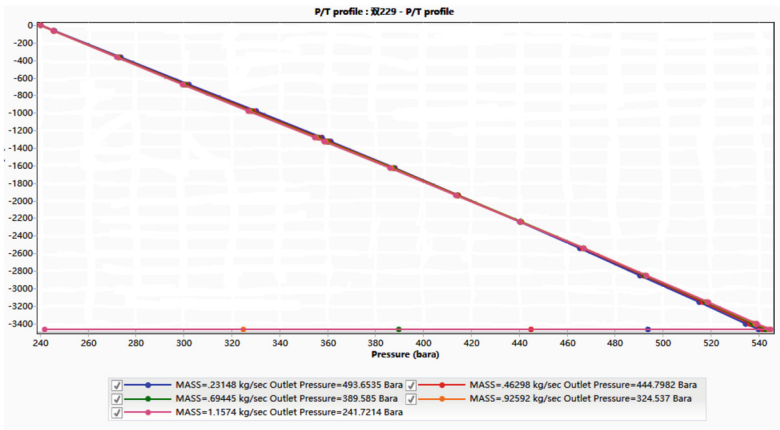


Fig. 18. Wellbore pressure prediction chart

4.4 Research of Matched Technology

4.4.1 Injection String

P110 steel pipe is used on the premise that no water is contained in the injection process, continuous gas injection is maintained or corrosion inhibitor is added to the wellbore when the injection is stopped. The packer shall select a removable gas seal with a pressure resistance of 70 MPa and temperature resistance of 140 °C, the rubber parts shall be made of hydrogenated nitrile butadiene rubber and the buckle type adopts the gas seal thread buckle to protect the casing above the oil layer from long-term corrosion, the depth of the packer shall be as close to the top of the oil layer as possible under the conditions of the packer and the existing operating capacity. Pipe string adopts general gas injection pipe string, as shown in Fig. 20.

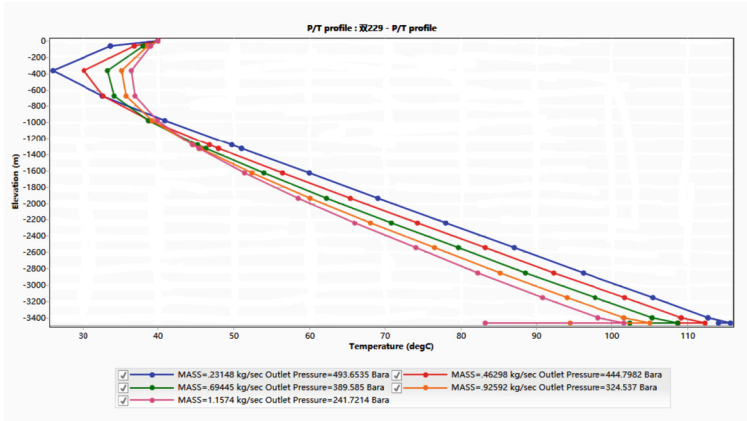


Fig. 19. Wellbore temperature prediction chart

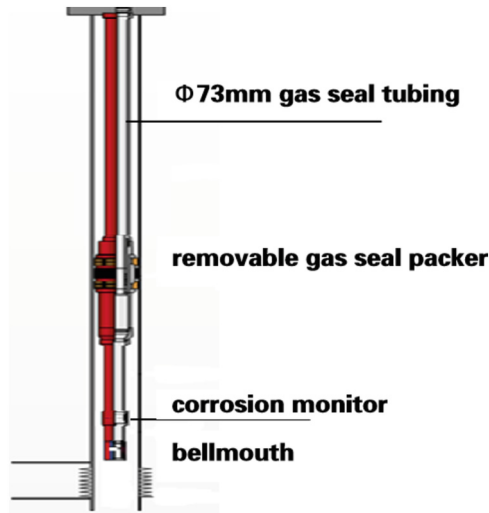


Fig. 20. Schematic diagram of the gas injection string

4.4.2 Lifting Technology

The swabbing parameters of reservoir engineering allocation are designed with a diameter of $\Phi 38$ mm pump, a stroke of 5 m and a stroke of 3 min^{-1} . At the same time, considering the requirement of high gas-liquid lifting in the later stage, considering the requirement of high gas-liquid ratio of CO₂ flooding, the lifting process of anti-corrosion anti-gas pump and composite gas anchor is selected to meet the lifting requirement of gas-liquid ratio >500 . At the same time, considering the influence of corrosion in the lifting process, the wellhead drip injection process of preservative was adopted, and the preservative concentration was controlled at 0.6% (Table 4).

Table 4. Lifting string design with different gas-liquid ratios

Lifting string design	Suitable gas-liquid ratio	Performance parameter
Anti-corrosion and anti-air pump + centrifugal gravity composite settling gas anchor	>500	Comprehensive corrosion rate ≤ 0.045 mm The maximum theoretical displacement is 35 t/d Sleeve pressure ≥ 2 MPa

5 Field Test of Shuang229 Block

Up to now, a total of 9 well groups were injected in Shuang229 blocks, the cumulative injection of carbon dioxide is 35 thousand tons. The efficiency of the front well was 48%, and the oil increase ranged from 2 to 8 tons in a single well, which achieved a good stimulation effect (Fig. 21).

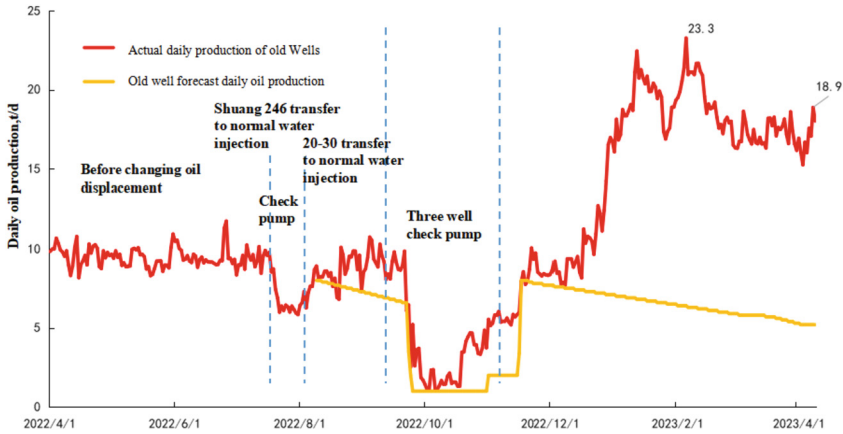


Fig. 21. Production data after CO₂ injection

6 Conclusion

- 1) Shuang229 block is a low permeability and deep buried hill reservoir, which is difficult to use for water-flooding development. The formation energy can be effectively supplemented after the implementation of carbon dioxide flooding, and the corresponding production well has obvious effect. Therefore, carbon dioxide flooding is a feasible EOR technology for low permeability and high pressure water-flooding reservoirs that are difficult to use.
- 2) The energy increase, swelling and viscosity reduction of carbon dioxide and the improvement of oil washing efficiency are integrated together, so that the oil flooding effect is better than that of water flooding and oxygen reducing air flooding.

- 3) Gas seal injection, gas lift prevention and production corrosion prevention are the three core technologies in the process of carbon dioxide flooding. Liaohe Oilfield has formed a mature supporting technology to ensure the smooth implementation of the pilot test.

References

1. Dai, Z., et al.: An integrated framework for optimizing CO₂ sequestration and enhanced oil recovery. *Environ. Sci. Technol. Lett.* **1**, 49–54 (2014)
2. Bachu, S.: Identification of oil reservoirs suitable for CO₂-EOR and CO₂ storage (CCUS) using reserves databases, with application to Alberta, Canada. *Int. J. Greenh. Gas Control* **44**, 152–165 (2016)
3. Tapia, J.F.D., Lee, J.-Y., Ooi, R.E., Foo, D.C., Tan, R.R.: Optimal CO₂ allocation and scheduling in enhanced oil recovery (EOR) operations. *Appl. Energy* **184**, 337–345 (2016)
4. Ghedan, S.G.: Global laboratory experience of CO₂-EOR flooding. In: *Proceedings of the SPE/EAGE Reservoir Characterization and Simulation Conference*, Abu Dhabi, United Arab Emirates, 19–21 October 2009
5. Zhao, Y., Rui, Z., Zhang, Z., et al.: Importance of conformance control in reinforcing synergy of CO₂ EOR and sequestration. *Petrol. Sci.* **19**(06), 3088–3106 (2022)
6. Jacob, E., Karl, T., Marion, M., et al.: Carbon dioxide flooding to reduce postoperative neurological injury following surgery for acute type a aortic dissection: a prospective, randomised, blinded, controlled clinical trial, CARTA study protocol - objectives and design. *BMJ Open* **13**(5) (2023)
7. Ruofei, W., Heng, Z., Xingbo, W., et al.: Designing a microfluidic chip driven by carbon dioxide for separation and detection of particulate matter. *Micromachines* **14**(1) (2023)
8. Xueqin, X., Qiao, D., Pengfei, S., et al.: Low-carbon oil exploitation: carbon dioxide flooding technology. *Frontiers Earth Sci.* (2023)
9. Xiaoyan, P., Chunyu, T., Yanning, W., et al.: CO₂-driven reversible transfer of amine-functionalized ZIF-90 between organic and aqueous phases. *Chem. Commun. (Cambridge England)* (2022)
10. Wang, F., Jia, J., Tian, X.: Suppression of methane explosion in pipeline network by carbon dioxide-driven calcified montmorillonite powder. *Arab. J. Chem.* **15**(10) (2022)
11. Yi, Z., Bin, Z., Yongzhi, Y., et al.: Storage ratio of CO₂ miscible flooding in Chang 8 reservoir of H block in ordos basin under different injection methods. *Frontiers Energy Res.* **10** (2022)
12. Yuejun, Z., Guangjuan, F., Kaoping, S., et al.: The experimental research for reducing the minimum miscibility pressure of carbon dioxide miscible flooding. *Renew. Sustain. Energy Rev.* **145** (2021)
13. Niu, Q., Wang, W., Liang, J., et al.: Investigation of the CO₂ flooding behavior and its collaborative controlling factors. *Energy Fuels* **34**(9) (2020)
14. Feng, S., Lin, Y.: Development of dissolved carbon dioxide-driven-and-controlled repeated batch fermentation process for ethanol production. *Can. J. Chem. Eng.* **98**(12) (2020)
15. Hu, Y., Hao, M., Chen, G., et al.: Technologies and practice of CO₂ flooding and sequestration in China. *Petrol. Exp. Dev. Online* **46**(4) (2019)